In silico Analysis of Anti-asthmatic Potential of Phytochemicals from Moringa oleifera against S-nitrosoglutathione reductase and Interleukin-13

***Bello, I.A.[1], Abdul-Hammed, M.[2], Akintoye, J.O.[1], Ismail, U.T.[2] and Salis, M.A.[2]**
[1] Physical Chemistry Unit, Department of Pure and Applied Chemistry,
Ladoke Akintola University of Technology, LAUTECH, Ogbomoso.
[2] Computational/ Biophysical Chemistry Unit, Department of Pure and Applied Chemistry,
Ladoke Akintola University of Technology, LAUTECH, Ogbomoso.
*Corresponding author; iabello52@lautech.edu.ng
DOI: 10.56201/ijccp.v11.no1.2025.pg19.56

Abstract
Asthma and inflammatory diseases remain major global health challenges, necessitating the search for novel therapeutic agents. Conventional treatments often come with limitations such as side effects and resistance, highlighting the need for alternative solutions. Natural compounds derived from medicinal plants have gained attention for their potential in drug discovery due to their diverse bioactive properties. Moringa oleifera is widely known for its medicinal properties, including its anti-inflammatory and antioxidant effects. This study employed computer-aided drug design to evaluate the effectiveness of phytochemicals derived from Moringa oleifera as potential inhibitors of GSNOR (PDB ID: 3QJ5) and IL-13 (PDB ID: 5L6Y). Reported phytochemicals isolated from Moringa oleifera were screened via molecular docking simulation using the PyRx docking tool against S-Nitrosoglutathione Reductase (GSNOR) (PDB ID: 3QJ5) and Interleukin-13 (IL-13) (PDB ID: 5L6Y), followed by ADMET profiling, drug-likeness, oral bioavailability, and bioactivity profiles. The results identified fucosterol (-8.8 kcal/mol), cholest-5-en-3-ol (-8.6 kcal/mol), ketocampesterol (-8.4 kcal/mol), ketositosterol (-8.3 kcal/mol), and poriferasterol (-8.2 kcal/mol) as potent inhibitors of GSNOR , while Fucosterol (-7.7 kcal/mol), Luteolin (-7.2 kcal/mol), and Flavylium (-7.2 kcal/mol) exhibited strong binding affinities against IL-13. These compounds demonstrated better interactions compared to the standard drugs Hydrocortisone (-7.8 kcal/mol) and Theophylline (-5.7 kcal/mol) against GSNOR and Hydrocortisone (-6.1 kcal/mol) and Theophylline (-4.4 kcal/mol) against IL-13, indicating their potential as effective inhibitors. Additionally, they possessed favorable ADMET properties, including good oral absorption, low toxicity, and high bioavailability. This research implied that the phytochemicals from M. oleifera are rich in bioactive compounds useful in the management of asthma. Therefore, the lead compounds are hereby recommended as potential drug candidates for further drug design processes.

Keywords: *Moringa oleifera; Asthma, Drug discovery; Phytochemicals; S-Nitrosoglutathione Reductase (GSNOR); Interleukin-13 (IL-13).*

1. **Introduction**

Asthma is a chronic inflammatory disease of the airways, about 262 million people are affected by asthma and caused 461,000 deaths in the year 2019 (WHO, 2020), and poses a significant burden on healthcare systems and quality of life. The disease is characterized by airway hyperresponsiveness, inflammation, and remodeling, driven by complex molecular pathways involving cytokines, enzymes, and oxidative stress (Adigwe *et al.*, 2022). Chronic asthma develops in approximately 70% of affected individuals, with a range of 50–85%, and can lead to severe complications such as airway remodeling and respiratory failure (Barnes, 2022). Despite advancements in asthma management, current therapies, including corticosteroids and β2-agonists, are associated with side effects such as immunosuppression, osteoporosis, and drug resistance (Vithi *et al.*, 2023). These limitations highlight the urgent need for novel therapeutic agents with improved efficacy and safety profiles.

Moringa oleifera, commonly referred to as the drumstick tree, is widely known for its diverse pharmacological benefits, including antioxidant, anti-inflammatory, and immunomodulatory activities (Anuragi *et al.*, 2022). Several studies have suggested that its bioactive constituents, including flavonoids, alkaloids, and terpenoids, may contribute to respiratory health by modulating inflammatory pathways and oxidative stress (Mahajan *et al.*, 2009). However, a systematic investigation into its potential molecular interactions with key asthma-related targets is crucial to understanding its therapeutic potential.

Among the molecular targets implicated in asthma pathogenesis, S-nitrosoglutathione reductase (GSNOR, PDB ID: 3QJ5) and Interleukin-13 receptor (IL-13R, PDB ID: 5L6Y) play crucial roles. GSNOR is involved in regulating S-nitrosothiols, which contribute to airway smooth muscle relaxation and inflammation (Sun et al., 2011). Dysregulation of GSNOR has been linked to increased airway hyperresponsiveness and asthma severity (Barnett & Buxton 2017). IL-13, a key Th2 cytokine, is central to airway inflammation, mucus production, and fibrosis in asthma patients (Popovic, 2016). Inhibiting IL-13R has been explored as a therapeutic strategy to reduce asthma symptoms and improve lung function (Panettieri *et al.*, 2018).

Advances in in silico drug discovery, particularly Computer-Aided Drug Design (CADD), have enabled rapid identification of promising drug candidates by integrating molecular docking, virtual screening, and pharmacokinetic analysis (Lee *et al.*, 2019). Molecular docking predicts the binding affinity and interactions of bioactive compounds within target proteins, providing insights into their potential therapeutic effects. ADMET (Absorption, Distribution, Metabolism, Excretion, and Toxicity) analysis and drug-likeness analysis ensures that candidate compounds possess favorable pharmacokinetic properties, reducing the likelihood of drug failure in later development stages (Daina et al., 2017).

Therefore, this study employs in silico approaches, including molecular docking, ADMET profiling, drug-likeness evaluation, bioactivity prediction, oral bioavailable analysis and molecular interaction, to investigate the potential of *Moringa oleifera* phytochemicals against GSNOR (PDB ID: 3QJ5) and IL-13R (PDB ID: 5L6Y).

2. Materials and methods

2.1. Preparation of ligands

A total of 177 isolated phytochemicals from *Moringa oleifera* were used for this study. These phytochemicals were categorized into various classes, including 49 alkaloids, 43 flavonoids, 12 phenolic acids, 18 steroids, and 55 terpenoids from *Moringa oleifera.* Additionally, two standard drugs, Theophylline and Hydrocortisone, were included for comparative analysis. The 2D/3D structures of the ligands and standard drugs were retrieved from the PubChem database (https://pubchem.ncbi.nlm.nih.gov/), and converted to 3D structures using Spartan 14 software. A conformational search was also carried out using Spartan'14 as well as molecular mechanics (MMFF) in which the stable conformers were carefully selected and optimized using density functional theory method (DFT) with B3LYP and 6-3+G(*) as a basis, to obtain structures with the best equilibrium geometry before molecular simulations.

2.2. Preparation of the Target receptor

The crystal structures of S-nitrosoglutathione reductase (GSNOR) (PDB ID: 3QJ5) and interleukin-13 in complex with tralokinumab (PDB ID: 5L6Y) were retrieved from the Protein Data Bank (RCSB) (http://www.rcsb.org/pdb). GSNOR is a key enzyme that regulates intracellular levels of S-nitrosoglutathione (GSNO) and protein S-nitrosothiols, playing a critical role in nitric oxide metabolism, smooth muscle relaxation, immune response, and inflammation (Barnett & Buxton, 2017). Interleukin-13 (IL-13) is a cytokine involved in asthma pathogenesis, and tralokinumab is an IL-13-neutralizing monoclonal antibody with demonstrated therapeutic efficacy (Popovic et al., 2017).

2.3 Determination of receptors' active sites

The binding pockets, ligand interactions, and amino acids in the active sites of 3QJ5 and 5L6Y were identified using the Computer Atlas for Surface Topography of Proteins (CASTP) (http://sts.bioc.uic.edu/castp) (Tian et al., 2018) and Biovia Discovery Studio (2019) (BIOVIA, 2019). The results were validated against previously reported experimental data on the active sites and residues of these receptors.

A **B**

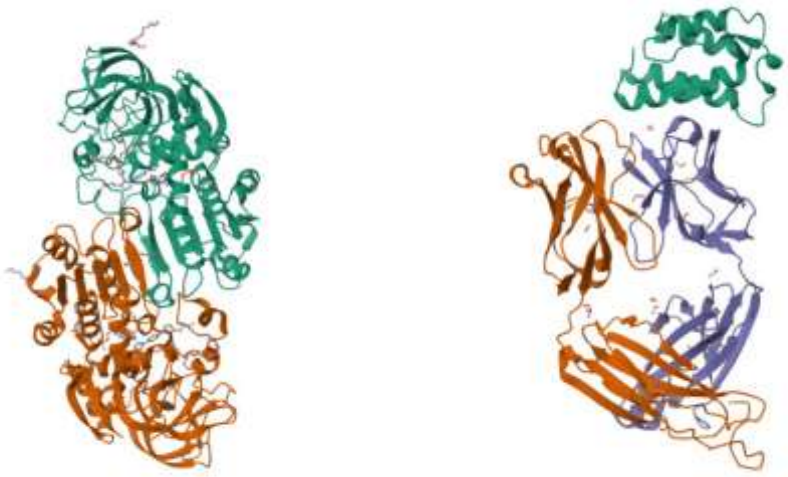

Figure1: The crystal structure (A) S-nitrosoglutathione Reductase Inhibitor (PDB ID: 3QJ5) and (B) Interleukin-13 in complex with Tralokinumab (PDB ID: 5L6Y)

2.4. Molecular Docking Protocol

Water molecules, heteroatoms, and other non-protein complexes were removed from the receptor structures (PDB IDs: 3QJ5 and 5L6Y) using Biovia Discovery Studio 4.5 Client. Molecular docking simulations were performed using PyRx, a virtual screening tool equipped with Open Babel and AutoDock Vina. The grid box dimensions were set to 36.37 Å × 42.07 Å × 61.93 Å (x, y, z axes), with a grid center at 23.00 Å × 47.19 Å × 59.35 Å and a spacing of 1.000 Å. The inhibition constants (Ki) in µM of the ligands and the standard method were obtained using their binding affinities (ΔG) in kcal/mol as shown in (equation 1) below, thus showing their potency against the target receptors (3QJ5 and 5L6Y).

$K_i = \exp(\Delta G/RT)$ (1)

Where R= Gas constant(1.987×10^{-3} kcal/mol); T=298.15K (absolute temperature);
K_i= Inhibition constant and ΔG = Binding energy

2.5. ADMET profiling, Drug likeness analysis and other analyses

The absorption, distribution, metabolism, excretion, and toxicity (ADMET) properties of the ligands were predicted using the ADMETsar2 web server (https://lmmd.ecust.edu.cn/admetsar2/) (Cheng et al., 2012). This tool provided insights into the pharmacokinetic and pharmacodynamic profiles of the ligands, ensuring their suitability as potential drug candidates. The drug-like properties and oral bioavailability assessmentsof the phytochemicals and standard drugs were evaluated using the Swiss-ADME web server (http://www.swissadme.ch/) (Daina et al., 2017). Lipinski's rule of five (RO5) was applied to assess drug-likeness, allowing no more than one violation of the following criteria: molecular weight (MW) ≤ 500 Da, hydrogen bond donors (HBDs) ≤ 5, hydrogen bond acceptors (HBAs) ≤ 10, and octanol-water partition coefficient (log P) ≤ 5 (Lipinski, 2004).

3. **Results and Discussion**

3.1. Structural and active site analysis of the target receptors

3.1.1.S-Nitrosoglutathione Reductase (GSNOR)

The X-ray crystallographic structure of S-nitrosoglutathione reductase (GSNOR) (PDB ID: 3QJ5) (Figure. 1) contains 374 amino acid residues complexed with a cofactor N6022 (NAD+). The resolution of the protein, as revealed by X-ray diffraction, was 1.90 Å, with crystal dimensions of a = 78.858 Å, b = 78.858 Å, and c = 310.078 Å, and angles α (90°), β (90°), and γ (90°), respectively. The R-values (free, work, and observed) are 0.210, 0.184, and 0.185, respectively. GSNOR is a key enzyme that regulates intracellular levels of S-nitrosoglutathione (GSNO), a critical mediator of nitric oxide (NO) signaling. By catalyzing the irreversible conversion of GSNO to oxidized glutathione, GSNOR plays a pivotal role in modulating smooth muscle relaxation, immune response, and inflammation (Barnett & Buxton, 2017). Dysregulation of GSNOR activity has been implicated in various inflammatory diseases, including asthma, where excessive NO production contributes to airway hyperresponsiveness and inflammation. The active site residues of GSNOR include Amino acid residue at the active site as follows, Cys 44, His 45, Thr 46, Tyr 49, His 66, Lys 81, Tyr 9, Ile 93, Gln 95, Cys 96, Cys 99, Arg 114, Lys 283, Gln 111, Cys 173,Gln 117, which are critical for NAD+ binding and catalytic activity (Sun et al., 2011).

3.1.2.Interleukin-13 (IL-13) in Complex with Tralokinumab

The X-ray crystallographic structure of interleukin-13 (IL-13) in complex with tralokinumab (PDB ID: 5L6Y) (Figure. 1) contains 112 amino acid residues. The resolution of the protein, as revealed by X-ray diffraction, was 1.99 Å, with crystal dimensions of a = 50.998 Å, b = 53.195 Å, and c = 62.05 Å, and angles α (107.91°), β (101.42°), and γ (96.94°), respectively. The R-values (free, work, and observed) are 0.211, 0.189, and 0.190, respectively. IL-13 is a cytokine that plays a central role in the pathogenesis of asthma by promoting eosinophilic inflammation, mucus hypersecretion, and airway remodeling (Popovic et al., 2017). Tralokinumab, an IL-13-neutralizing human IgG4 monoclonal antibody, binds to IL-13 and prevents its interaction with the IL-13 receptor, thereby inhibiting downstream signaling pathways. The active site residues of IL-13 involved in tralokinumab binding include Asp50, Lys31, Ser30, Asp51, Asn26, Gly81, Asp92, Arg 107, Lys 104, Lys 103, which are critical for receptor recognition and neutralization (Popovic et al., 2017).

3.2. Molecular Docking Analysis of Phytochemicals Against GSNOR and IL-13 Receptors

The process of drug discovery involves identifying compounds that interact effectively with target proteins to modulate biological functions. Traditional drug discovery methods are time-intensive, costly, and have a high failure rate. Computer-Aided Drug Design (CADD) techniques, such as molecular docking, provide a cost-effective alternative by predicting ligand-receptor interactions and estimating their binding strength. Molecular docking evaluates binding affinity using binding energy (BE, kcal/mol) and inhibition constant (Ki, µM), where lower values indicate stronger interactions (Falade *et al.,* 2021). A total of 177 ligands were screened against S-nitrosoglutathione reductase (GSNOR, PDB ID: 3QJ5) and Interleukin-13 (IL-13, PDB ID: 5L6Y) to evaluate their binding affinity using molecular docking. Those that have higher binding affinity than the standards were shown in the Table 3.1 and 3.2 respectively, Lutein exhibited the highest binding affinity with a docking score of -12.4 kcal/mol and an inhibition constant (Ki) of 0.00082 µM, indicating a strong interaction with the target protein.

Other carotenoids such as All-trans-Neoxanthin (-10.4 kcal/mol, Ki = 0.024 µM), Alpha-Carotene (-10.3 kcal/mol, Ki = 0.028 µM), and Beta-Carotene (-10.0 kcal/mol, Ki = 0.047 µM) also demonstrated significant binding affinity. Notably, flavonoids such as Isoorientin (-9.7 kcal/mol, Ki = 0.078 µM), Epigallocatechin gallate (-9.3 kcal/mol, Ki = 0.15 µM), and Luteolin 7-O-glucoside (-9.2 kcal/mol, Ki = 0.18 µM) exhibited promising interactions. Additionally, sterols including Lanosterol (-9.4 kcal/mol, Ki = 0.12 µM), 7-Dehydrostigmasterol (-9.2 kcal/mol, Ki = 0.18 µM), and Cycloartenol (-8.9 kcal/mol, Ki = 0.30 µM) showed moderate binding affinities. Comparatively, standard drugs such as Hydrocortisone (-7.8 kcal/mol, Ki = 1.92 µM) and Theophylline (-5.7 kcal/mol, Ki = 66.61 µM) exhibited weaker interactions, suggesting that several of the screened phytochemicals might serve as more potent inhibitors.

Molecular docking studies of phytochemicals from Moringa oleifera against the IL-13 receptor (PDB: 5L6Y) revealed promising interactions, with several compounds demonstrating strong binding affinities and low inhibition constants. Lutein exhibited the highest binding affinity (-9.7 kcal/mol) and the lowest inhibition constant (0.078 µM), suggesting a high potential for inhibitory activity. Other notable compounds include α-carotene and β-carotene, both with binding affinities of -9.0 kcal/mol and inhibition constants of 0.254 µM, as well as N-α-L-rhamnopyranosyl vincosamide (-8.8 kcal/mol, 0.357 µM). Epigallocatechin gallate (-8.0 kcal/mol, 1.375 µM) and zeaxanthin (-7.9 kcal/mol, 1.628 µM) also showed moderate binding, further supporting the potential of Moringa oleifera-derived phytochemicals as IL-13 receptor modulators. In contrast, standard r compounds such as hydrocortisone (-6.1 kcal/mol, 33.919 µM) and theophylline (-4.4 kcal/mol, 597.99 µM) displayed significantly weaker interactions, reinforcing the efficacy of the identified phytochemicals. These findings highlight the therapeutic potential of natural bioactive compounds in modulating IL-13-related pathways and warrant further investigation for potential applications in immune and inflammatory disorders.

Table 3.1 Docking scoring and inhibition constants of phytochemicals from *Moringa oleifera* with 3QJ5

S/N	LIGAND	BINDING AFFINITY (), kcal/mol	INHIBITION CONSTANT (Ki)
1	Lutein	-12.4	0.00082
2	All-trans-Neoxanthin	-10.4	0.024
3	Alpha-Carotene	-10.3	0.028
4	Beta-Carotene	-10	0.047
5	Isoorientin	-9.7	0.078
6	All-E-Zeaxanthin	-9.6	0.092
7	Homoorientin	-9.6	0.092
8	Roridin	-9.6	0.092
9	Violaxanthin	-9.6	0.092

10	Lanosterol	-9.4	0.12
11	Epigallocatechin_gallate	-9.3	0.15
12	7-Dehydrostigmasterol	-9.2	0.18
13	22-Dehydrocholesterol	-9.2	0.18
14	Bauerenol	-9.2	0.18
15	Luteolin_7-O-glucoside	-9.2	0.18
16	24-Methylenecycloartanol	-9.1	0.21
17	24-Ethylidenelophenol	-9	0.25
18	Hyperoside	-9	0.25
19	Pyrrolemarumine	-9	0.25
20	7-Dehydrocampesterol	-8.9	0.30
21	Cycloartenol	-8.9	0.30
22	Desmosterol	-8.9	0.30
23	Spinasterol	-8.9	0.30
24	Brassicasterol	-8.8	0.36
25	Campestanol	-8.8	0.36
26	Fucosterol	-8.8	0.36
27	Gramisterol	-8.8	0.36
28	24-Methylenelophenol	-8.7	0.42
29	Campesterol	-8.7	0.42
30	Cholesterol	-8.7	0.42
31	Clerosterol	-8.7	0.42
32	delta7-Avenasterol	-8.7	0.42
33	Sitostanol	-8.7	0.42
34	Stigmasterol	-8.7	0.42
35	Zeaxanthin	-8.7	0.42
36	7-Dehydrositosterol	-8.6	0.50
37	Astragalin	-8.6	0.50
38	beta-Sitostenone	-8.6	0.50

39	Cholest-5-en-3-ol	-8.6	0.50
40	Lathosterol	-8.6	0.50
41	Orientin	-8.6	0.50
42	7-Ketocholesterol	-8.5	0.59
43	28-isoavenasterol	-8.5	0.59
44	Cholestanol	-8.5	0.59
45	Ellagic_acid	-8.5	0.59
46	Ergosterol	-8.5	0.59
47	7-Ketocampesterol	-8.4	0.70
48	7-Ketostigmasterol	-8.4	0.70
49	22-Hydroxycholesterol	-8.4	0.70
50	Aurantiamide_acetate	-8.4	0.70
51	Morin	-8.4	0.70
52	Quercetagetin	-8.4	0.70
53	7-Ketositosterol	-8.3	0.83
54	20-Hydroxycholesterol	-8.3	0.83
55	Flavylium	-8.3	0.83
56	Gossypetin	-8.3	0.83
57	Kaempferol	-8.3	0.83
58	Quercetin	-8.3	0.83
59	24-Ethylcholesterol	-8.2	0.98
60	24-Hydroxycholesterol	-8.2	0.98
61	Poriferasterol	-8.2	0.98
62	Scutellarein	-8.2	0.98
63	Diosmetin	-8.1	1.16
64	Pratensein	-8.1	1.16
65	(-)-Epicatechin	-8	1.37
66	beta-Sitosterol	-8	1.37
67	Biochanin	-8	1.37

68	Chrysoeriol	-8	1.37
69	Genistein	-8	1.37
70	Luteolin	-8	1.37
71	Cianidanol	-7.9	1.63
72	1_3-Dibenzyl_urea	-7.8	1.92
73	6-Chromanol	-7.8	1.92
74	Chrysin	-7.8	1.92
75	Hesperetin	-7.8	1.92
76	**Hydrocortisone_STANDARD**	**-7.8**	**1.92**
77	**Theophylline_STANDARD**	**-5.7**	**66.61**

Table 3.2 Docking score and inhibition constants of phytochemicals from Moringa oleifera with 5L6Y

S/N	Ligand	Binding Affinity	Inhibition Constant
1	Lutein	-9.7	0.07
2	alpha-Carotene	-9	0.25
3	beta-Carotene	-9	0.25
4	Nalpha-L-rhamnopyranosyl_vincosamide	-8.8	0.35
5	Epigallocatechin_gallate	-8	1.37
6	Zeaxanthin	-7.9	1.62
7	Isofucosterol	-7.8	1.92
8	all-trans-Neoxanthin	-7.7	2.28
9	Fucosterol	-7.7	2.28
10	24-Methylene_cholesterol	-7.6	2.70
11	All-E-Zeaxanthin	-7.6	2.70
12	7-Ketocampesterol	-7.5	3.19
13	Cycloartenol	-7.5	3.19
14	Clerosterol	-7.4	3.78
15	20-Hydroxycholesterol	-7.3	4.47
116	24-Methylenecycloartanol	-7.2	5.30
17	Flavylium	-7.2	5.30
18	Luteolin_7-O-glucoside	-7.2	5.30
19	Rutin	-7.2	5.30
20	Bauerenol	-7.1	6.27

21	7-Dehydrostigmasterol	-7.1	6.27
22	22-Dehydrocholesterol	-7.1	6.27
23	Lanosterol	-7.1	6.27
24	Sitostanol	-7.1	6.27
25	7-Dehydrocampesterol	-7	7.43
26	7-Ketositosterol	-7	7.43
27	24-Ethylidenelophenol	-7	7.43
28	Brassicasterol	-7	7.43
29	Cholestanol	-7	7.43
30	delta7-Avenasterol	-7	7.43
31	Poriferasterol	-7	7.430
32	Stigmasterol	-7	7.43
33	7-Dehydrocholesterol	-6.9	8.79
34	beta-Sitosterol	-6.9	8.79
35	Pterygospermin	-6.9	8.79
36	6-Chromanol_2,8-dimethyl-2-(4,8,12-trimethyltridecyl)	-6.8	10.41
37	7-Dehydrositosterol	-6.8	10.41
38	7-Ketocholesterol	-6.8	10.41
39	22-Hydroxycholesterol	-6.8	10.41
40	Desmosterol	-6.8	10.41
41	Roridin_E	-6.8	10.41
42	7-Ketostigmasterol	-6.7	12.32
43	Campesterol	-6.7	12.32
44	Cholest-5-en-3-ol	-6.7	12.32
45	Cholesterol_1	-6.7	12.32
46	Ergosterol	-6.7	12.32
47	Lathosterol	-6.7	12.32
48	Lycopene	-6.7	12.32
49	24-Methylenelophenol	-6.6	14.59
50	beta-Sitostenone	-6.6	14.59
51	Campestanol	-6.6	14.59
52	Gramisterol	-6.6	14.59
53	Violaxanthin	-6.6	14.59
54	4-Hydroxyphenyl_acetonitrile	-6.5	17.27
55	Chrysin	-6.5	17.27
56	Epiglobulol	-6.5	17.27
57	Homoorientin_1	-6.5	17.27
58	Isoorientin	-6.5	17.27
59	Orientin	-6.5	17.27
60	Scutellarein	-6.5	17.27

61	24-Ethylcholesterol	-6.4	20.44
62	24-Hydroxycholesterol	-6.4	20.44
63	ar-Turmerone	-6.4	20.44
64	Aurantiamide_acetate	-6.4	20.44
65	beta-Caryophyllene	-6.4	20.44
66	Genistein	-6.4	20.44
67	Gossypetin	-6.4	20.44
68	Pratensein	-6.4	20.44
69	Spathulenol	-6.4	20.44
70	Biochanin_A	-6.3	24.20
71	Diosmetin	-6.3	24.20
72	Ellagic_acid	-6.3	24.20
73	Fisetin	-6.3	24.20
74	Kaempferol	-6.3	24.20
75	Spinasterol	-6.3	24.20
76	Astragalin	-6.2	28.65
77	Chrysoeriol	-6.2	28.65
78	Morin	-6.2	28.65
79	Pyrrolemarumine	-6.2	28.65
80	Quercetin_	-6.2	28.65
81	alpha-Cadinol	-6.1	33.91
82	Carvacrol	-6.1	33.91
83	**Hydrocortisone_STANDARD**	**-6.1**	**33.91**
84	**Theophylline_STANDARD**	**-4.4**	**597.11**

3.3. ADMET (pharmacokinetics) analysis of the selected compounds

Absorption, Distribution, Metabolism, Excretion, and Toxicity (ADMET) profiling remains an indispensable step in the early stages of drug discovery. It plays a crucial role in understanding the pharmacokinetic properties of ligand molecules, ensuring that a potential drug candidate possesses both the required potency and efficacy while maintaining a reliable ADMET profile (Adedotun et al., 2022). The availability of ADMET data facilitates the selection of ligands with optimal safety profiles at therapeutic doses during the initial stages of drug discovery, thereby preventing unnecessary resource allocation to molecules that may ultimately be unsuitable for development. In this study, ADMET properties were predicted using the admetSAR web tool. A drug candidate is expected to exhibit favorable human intestinal absorption (HIA), aqueous solubility within the recommended range of Log S between -1 and -5, and non-inhibitory activity against cytochrome P450 enzymes. Additionally, the compound should not exhibit Ames toxicity, carcinogenicity, or HERG inhibition, and should have either no toxicity or only a low level of toxicity. The ADMET screening was conducted on the bioactive compounds that has higher binding affinity than the standards as shown in Tables 3.3. The findings indicate that 50 out of the selected bioactive compounds passed ADMET

profilling demonstrated positive human intestinal absorption (HIA+), suggesting their ability to be efficiently absorbed in the human intestine. Similarly, most of these compounds exhibited the ability to cross the blood-brain barrier (BBB+), further reinforcing their favorable distribution properties. The aqueous solubility values of all selected compounds fell within the recommended range, aligning with established pharmacokinetic guidelines (Abdul-Hammed et al., 2021).

The metabolic activity of the selected compounds was assessed by evaluating their interaction with cytochrome P450 enzymes, which are critical for drug metabolism. As expected, nearly all selected compounds were identified as non-inhibitors of the examined CYP450 enzymes, indicating a lower likelihood of metabolic interference. Furthermore, none of the selected compounds exhibited Ames toxicity, and they were classified as possessing either Type IV (non-toxic) or Type III (slightly toxic) acute oral toxicity properties. Notably, compounds with Type III toxicity could be further optimized to achieve Type IV (non-toxic) status in the lead optimization stage of drug discovery.(Onawole *et al.*, 2017)

Table 3.3: ADMET Analysis of the studied phytochemicals from *Moringa oleifera*

	L1	**L2**	**L3**	**L4**	**L5**	**L6**	**L7**	**L8**	**L9**	**L10**
Absorption and distribution										
BBB(±)	-0.5331	+0.9779	+0.9469	+0.9749	+0.9743	+0.9825	+0.9280	+0.9645	+0.9817	+0.9675
HIA +	+0.96554	+0.9873	+1.0000	+1.0000	+1,0000	+1.0000	+1.0000	+0.9935	+0.9964	+1.0000
Aqueous Solubility (LogS)	-3.10	-2,654	-4.599	-4.809	-4.702	-4.683	-4.763	-4.723	-4.623	-5.446
Metabolism										
CYP4502C19 Inhibitor	-0.9041 Non-inhibitor	+0.5182 Inhibitor	-0.8107 Non-Inhibitor	-0.9177 Non-Inhibitor	-0.9025 Non-inhibitor	-0.7681 Non-inhibitor	-0.9214 Non-inhibitor	-0.7285 Non-inhibitor	-0.7480 Non-inhibitor	+0.6666 Inhibitor
CYP4501A2 Inhibitor	-0.9046 Non-inhibitor	-0.7774 Non-Inhibitor	-0.8907 Non-Inhibitor	-0.9355 Non-Inhibitor	-0.9291 Non-Inhibitor	-0.9088 Non-Inhibitor	-0.9180 Non-inhibitor	-0.8045 Non-Inhibitor	-0.9054 Non-Inhibitor	-0.9277 Non-inhibitor
CYP4503A4 Inhibitor	-0.6345 Non-inhibitor	-0.5883 Non-Inhibitor	-0.8517 Non-Inhibitor	-0.8638 Non-Inhibitor	-0.8309 Non-inhibitor	-0.8640 Non-inhibitor	-0.8392 Non-inhibitor	-0.8015 Non-inhibitor	-0.8499 Non-inhibitor	-0.8659 Non-inhibitor

CYP450 2C9 Inhibitor	-0.8227 Non-inhibitor	+0.5805 Inhibitor	-0.9270 Non-Inhibitor	-0.9194 Non-Inhibitor	-0.9125 Non-inhibitor	-0.8612 Non-inhibitor	-0.9511 Non-inhibitor	-0.7064 Non-inhibitor	-0.8492 Non-inhibitor	-0.8900 Non-inhibitor
CYP450 2D6 Inhibitor	-0.9231 Non-inhibitor	-0.8997 Non-inhibitor	-0.9429 Non-inhibitor	-0.9519 Non-inhibitor	-0.9346 Non-Inhibitor	-0.9483 Non-Inhibitor	-0.9476 Non-inhibitor	-0.9424 Non-inhibitor	-0.9460 Non-inhibitor	-0.9467 Non-inhibitor
Excretion										
Biodegradation	+0.7895 NB	-0.8947 NB	-0.9871 NB	-0.9825 NB	-0.9802 NB	+0.9861 NB	+0.9838 NB	-0.9960 NB	+0.9903 NB	+0.9659 NB
AMES Mutagenesis	-0.7658 Non-Ames toxic	-0.6593 Non-Ames toxic	-0.7963 Non-Ames toxic	-0.8888 Non-Ames toxic	-0.9132 Non-Ames toxic	-0.8954 Non-Ames toxic	-0.7719 Non-Ames toxic	-0.7110 Non-Ames toxic	-0.9172 Non-Ames toxic	-0.9384 Non-Ames toxic
Acute Oral Toxicity	IV 0.6433	III 0.7688	III 0.6859	I 0.5508	I 0.4287	III 0.8086	I 0.6104	III 0.7744	III 0.8414	III 0.8629
Eye irritation (YES/NO)	Yes	Yes	No	Yes	Yes	Yes	No	Yes	Yes	Yes
Eye corrosion (YES/NO)	No	No	No	Yes	Yes	Yes	No	Yes	Yes	No
hERG inhibition	-0.9666 No	-0.8590 No	-0.8189 No	-0.7730 No	-0.8027 No	-0.7863 No	-0.8070 No	-0.8908 No	-0.7864 No	-0.8412 No
Hepatotoxicity	-0.7487 No	-0.8286 No	-0.7523 Yes	-0.7552 No	-0.7104 No	-0.7617 No	-0.7492 No	-0.7483 No	-0.7991 No	-0.7896 No
Carcinogenicity (Yes/No)	-0.9539 No	-0.8439 No	-0.9277 No	-0.9320 No	-0.9182 No	-0.9335 No	-0.9256 No	-0.9261 No	-0.9288 No	-0.8984 No
Absorption and distribution										
	L11	**L12**	**L13**	**L14**	**L15**	**L16**	**L17**	**L18**	**L19**	**L20**

BBB(±)	+0.9749	-0.9743	-0.9617	-0.9615	+0.6588	+0.5866	+0.9399	+0.9455	+0.9647	+0.9455
HIA +	+1.0000	+1.0000	+1.0000	+1.0000	+0.9972	+0.9074	+0.9934	+1.0000	+0.9963	+1.0000
Aqueous Solubility (LogS)	-4.809	-4.073	-4.601	-4.533	-3.212	-3.095	-4.937	-3.909	-4.953	-5.054
Metabolism										
CYP4502C19 Inhibitor	-0.9177 Non-inhibitor	-0.9025 Non-Inhibitor	-0.9042 Non-Inhibitor	+0.8821 Inhibitor	+0.5225 Inhibitor	-0.6235 Non-inhibitor	-0.9033 Non-inhibitor	-0.6108 Non-inhibitor	-0.7868 Non-inhibitor	-0.5547 Non-inhibitor
CYP4501A2 Inhibitor	-0.9355 Non-inhibitor	-0.9291 Non-Inhibitor	-0.9516 Non-Inhibitor	+0.9484 Non-Inhibitor	-0.9079 Non-Inhibitor	-0.8214 Non-Inhibitor	+0.7359 Inhibitor	-0.8334 Non-Inhibitor	-0.9109 Non-Inhibitor	-0.8244 Non-inhibitor
CYP4503A4 Inhibitor	-0.8638 Non-inhibitor	-0.8309 Non-Inhibitor	-0.8603 Non-Inhibitor	+0.8167 Non-Inhibitor	-0.8808 Non-inhibitor	-0.7768 Non-inhibitor	-0.9377 Non-inhibitor	-0.8359 Non-inhibitor	-0.9290 Non-inhibitor	-0.8317 Non-inhibitor
CYP4502C9 Inhibitor	-0.9194 Non-inhibitor	-0.9125 Non-inhibitor	-0.9359 Non-Inhibitor	-0.9299 Non-Inhibitor	-0.7723 Non-inhibitor	-0.7617 Non-inhibitor	-0.8952 Non-inhibitor	-0.7000 Non-inhibitor	-0.8592 Non-inhibitor	-0.6749 Non-inhibitor
CYP4502D6 Inhibitor	-0.9519 Non-inhibitor	-0.9346 Non-inhibitor	-0.9583 Non-inhibitor	-0.9408 Non-inhibitor	-0.9368 Non-Inhibitor	-0.9298 Non-Inhibitor	-0.9423 Non-inhibitor	-0.9371 Non-inhibitor	-0.9444 Non-inhibitor	-0.9197 Non-inhibitor
Excretion										
Biodegradation	-0.9825 NB	+0.9802 B	-0.89658 NB	-0.9614 NB	+0.9655 B	+0.9682 B	+0.6228 B	-0.9531 NB	-0.8038 NB	-0.72744 NB
AMES Mutagenesis	-0.8888 Non-Ames toxic	-0.9132 Non-	-0.8470 Non-	-0.8766 Non-	-0.8391 Non-	-0.5818 Non-	-0.9373 Non-	-0.9157 Non-	-0.6543 Non-	-0.8588

		Ames toxic	Ames toxic	Ames toxic	Ames toxic	Ames toxic	Ames toxic	Ames toxic	Ames toxic	Non-Ames toxic
Acute Oral Toxicity	I 0.5508	I 0.4287	III 0.4950	III 0.5069	III 0.7696	III 0.3640	III 0.8619	III 0.8519	III 0.8007	III 0.7760
Eye irritation (YES/NO)	Yes	Yes	No	Yes	Yes	Yes	Yes	Yes	No	No
Eye corrosion (YES/NO)	Yes	Yes	No	No	Yes	Yes	Yes	No	No	No
hERG inhibition	-0.7730 No	-0.8027 No	-0.8621 No	-0.8819 No	-0.9273 No	-0.9776 No	-0.7372 No	-0.8709 No	-0.9132 No	-0.9122 No
Hepatotoxicity	-0.7522 No	-0.7104 No	-0.7795 No	-0.7407 No	-0.8259 No	-0.8989 No	-0.8327 No	-0.7046 No	-0.7908 No	-0.6809 No
Carcinogenicity (Yes/No)	-0.9320 No	-0.9182 No	-0.9342 No	-0.9210 No	-0.7489 No	-0.8890 No	-0.6621 No	-0.9094 No	-0.6907 No	-0.7830 No
Absorption and distribution										
	L21	**L22**	**L23**	**L24**	**L25**	**L26**	**L27**	**L28**	**L29**	**L30**
BBB(±)	-0.9733	+0.9369	-0.9415	+0.9505	+0.6975	+0.8572	+0.9618	+0.9406	-0.9455	+0.9647
HIA +	+0.9962	+1.0000	-0.9953	+1.0000	-0.7855	+0.9703	+1.0000	+0.9842	+1.0000	-0.9963
Aqueous Solubility (LogS)	-5.046	-5.346	-3.476	-3.199	-2.449	-2.419	-4.251	-5.015	-3.909	-4.953
Metabolism										
CYP4502C19 Inhibitor	-0.7952 Non-inhibitor	-0.7351 Non-Inhibitor	-0.9063 Non-Inhibitor	-0.7469 Non-Inhibitor	-0.9289 Non-inhibitor	-0.8291 Non-inhibitor	-0.6636 Non-inhibitor	-0.8653 Non-inhibitor	-0.6108 Non-Inhibitor	-0.7868 Non-inhibitor
CYP4501A2 Inhibitor	-0.8014 Non-inhibitor	-0.7484 Non-Inhibitor	-0.8015 Non-Inhibitor	-0.5650 Non-Inhibitor	-0.9084 Non-Inhibitor	-0.8955 Non-Inhibitor	-0.8575 Non-Inhibitor	-0.7209 Non-Inhibitor	-0.8334 Non-Inhibitor	-0.9109 Non-inhibitor

CYP450 3A4 Inhibitor	-0.9106 Non-inhibitor	-0.9426 Non-Inhibitor	-0.9581 Non-Inhibitor	-0.8097 Non-Inhibitor	-0.9194 Non-inhibitor	-0.5733 Non-inhibitor	-0.8699 Non-inhibitor	-0.9155 Non-inhibitor	-0.8359 Non-Inhibitor	-0.9290 Non-inhibitor
CYP450 2C9 Inhibitor	-0.7994 Non-inhibitor	-0.8378 Non-inhibitor	-0.9216 Non-Inhibitor	-0.8061 Non-Inhibitor	-0.9296 Non-inhibitor	-0.8759 Non-inhibitor	-0.7983 Non-inhibitor	-0.8744 Non-inhibitor	-0.7000 Non-Inhibitor	-0.8592 Non-inhibitor
CYP450 2D6 Inhibitor	-0.9406 Non-inhibitor	-0.9077 Non-inhibitor	-0.9312 Non-inhibitor	-0.9002 Non-inhibitor	-0.9513 Non-Inhibitor	-0.8585 Non-Inhibitor	-0.9399 Non-inhibitor	-0.9414 Non-inhibitor	-0.9371 Non-inhibitor	-0.9444 Non-inhibitor
Excretion										
Biodegradation	+0.8494 B	-0.6033 NB	+0.8391 B	+0.7554 B	-0.6295 NB	+0.5387 B	-0.9699 NB	+0.5180 B	-0.9531 NB	+0.8308 NB
AMES Mutagenesis	-0.9391 Non-Ames toxic	+0.5773 Ames toxic	-0.8892 Non-Ames toxic	-0.9682 Non-Ames toxic	+0.5776 Ames toxic	-0.7948 Non-Ames toxic	-0.8996 Non-Ames toxic	-0.9345 Non-Ames toxic	-0.9157 Non-Ames toxic	-0.6543 Non-Ames toxic
Acute Oral Toxicity	III 0.6889	III 0.6838	III 0.8506	III 0.7877	III 0.4045	III 0.6710	III 0.8299	III 0.9084	III 0.8519	III 0.8007
Eye irritation (YES/NO)	Yes	No	No	Yes	No	Yes	Yes	Yes	Yes	No
Eye corrosion (YES/NO)	Yes	No	No	No	No	Yes	No	Yes	No	No
hERG inhibition	-0.9169 No	-0.8502 Yes	-0.9010 No	-0.8356 No	-0.9813 Yes	-0.9931 No	-0.8351 No	-0.7328 No	-0.8709 No	-0.9132 No
Hepatotoxicity	-0.8474 No	-0.8502 No	-0.8996 No	-0.8591 No	-0.6865 No	-0.9333 No	-0.7513 No	-0.8499 No	-0.7046 No	-0.7908 No

Carcinogenicity (Yes/No)	-0.6532 No	-0.7717 No	-0.6199 No	-0.5168 No	-0.9589 No	-0.8055 No	-0.9227 No	-0.6510 No	-0.9094 No	-0.6907 No
Absorption and distribution										
	L31	**L32**	**L33**	**L34**	**L35**	**L36**	**L37**	**L38**	**L39**	**L40**
BBB(±)	+0.9536	+0.9425	+0.9817	+0.9743	-0.5674	+0.9667	+0.9719	+0.9642	-0.6632	+0.9876
HIA +	-0.9926	+0.9750	+1.0000	+1.0000	+0.9816	+0.9900	+0.9969	+1.0000	-0.9392	+0.9972
Aqueous Solubility (LogS)	-4.686	-5.254	-4.280	-4.703	-3.191	-2.979	-3.289	-4.692	-1.694	-4.548
Metabolism										
CYP4502C19 Inhibitor	-0.5957 Non-inhibitor	-0.8891 Non-Inhibitor	-0.6775 Non-Inhibitor	-0.9205 Non-Inhibitor	+0.9470 Inhibitor	-0.7863 Non-inhibitor	-0.7031 Non-inhibitor	-0.9025 Non-inhibitor	-0.9367 Non-Inhibitor	-0.8526 Non-inhibitor
CYP4501A2 Inhibitor	-0.6695 Non-inhibitor	-0.7161 Non-Inhibitor	-0.8768 Non-Inhibitor	-0.9291 Non-Inhibitor	+0.9540 Inhibitor	-0.7807 Non-Inhibitor	-0.9317 Non-Inhibitor	-0.9140 Non-Inhibitor	-0.9046 Non-Inhibitor	-0.7578 Non-inhibitor
CYP4503A4 Inhibitor	-0.8665 Non-inhibitor	-0.9627 Non-Inhibitor	-0.8747 Non-Inhibitor	-0.8309 Non-Inhibitor	+0.7746 Inhibitor	-0.8309 Non-inhibitor	-0.9384 Non-inhibitor	-0.8916 Non-inhibitor	-0.8869 Non-Inhibitor	-0.9020 Non-inhibitor
CYP4502C9 Inhibitor	-0.6249 Non-inhibitor	-0.8903 Non-inhibitor	-0.8798 Non-Inhibitor	-0.9125 Non-Inhibitor	+0.8287 Inhibitor	-0.7372 Non-inhibitor	-0.9218 Non-inhibitor	-0.9071 Non-inhibitor	-0.9071 Non-Inhibitor	-0.7690 Non-inhibitor
CYP4502D6 Inhibitor	-0.9284 Non-inhibitor	-0.9474 Non-inhibitor	-0.9416 Non-inhibitor	-0.9346 Non-inhibitor	-0.6939 Non-Inhibitor	-0.9392 Non-Inhibitor	-0.9606 Non-inhibitor	-0.9478 Non-inhibitor	-0.9525 Non-inhibitor	-0.9708 Non-inhibitor
Excretion										

Biodegradation	+0.5734 B	+0.7175 B	-0.9810 NB	-0.9802 NB	+0.8757 NB	-0.5749 NB	-0.5335 NB	-0.9623 NB	+0.8012 B	-0.9959 NB
AMES Mutagenesis	-0.9167 Non-Ames toxic	-0.9494 Non-Ames toxic	-0.9552 Non-Ames toxic	-0.9132 Non-Ames toxic	-0.9132 Non-Ames toxic	-0.8461 Non-Ames toxic	-0.9087 Non-Ames toxic	-0.9231 Non-Ames toxic	-0.9132 Non-Ames toxic	-0.8368 Non-Ames toxic
Acute Oral Toxicity	III 0.8200	III 0.9077	III 0.7154	I 0.4287	III 0.7005	III 0.8480	IV 0.4812	I 0.5416	IV 0.5588	III 0.8331
Eye irritation (YES/NO)	No	Yes	No	Yes	No	Yes	No	Yes	No	Yes
Eye corrosion (YES/NO)	No	Yes	No	No	No	Yes	No	Yes	No	Yes
hERG inhibition	-0.9225 No	-0.7690 No	-0.7701 No	-0.8027 No	-0.9521 No	-0.8314 No	-0.9483 No	-0.8502 No	-0.9763 No	-0.8855 No
Hepatotoxicity	-0.8537 No	-0.8720 No	-0.6984 No	-0.7104 No	-0.8682 No	-0.8059 No	-0.8556 No	-0.7488 No	-0.9548 No	-0.6000 No
Carcinogenicity (Yes/No)	-0.6863 No	+0.5698 Yes	-0.8193 No	-0.9182 No	-0.9347 No	-0.7739 No	-0.7995 No	-0.9287 No	-0.9183 No	-0.8914 No
Absorption and distribution										
	L41	**L42**	**L43**	**L44**	**L45**	**L46**	**L47**	**L48**	**L49**	**L50**
BBB(±)	+0.9750	+0.9500	+0.9250	+0.8250	-0.6500	+0.8000	+0.9750	-0.7500	+0.7250	-0.6500
HIA +	+0.9954	+0.9969	+0.9925	+0.9947	+0.9949	+1.0000	+0.9823	-0.6800	+0.9963	+0.8088
Aqueous Solubility (LogS)	-3.399	-3.239	-2.363	-4.040	-4.470	-4.308	-2.472	1.033	-2.417	-2.291
Metabolism										
CYP4502C19 Inhibitor	-0.9524 Non-inhibitor	-0.5241 Non-Inhibitor	-0.8903 Non-Inhibitor	-0.9467 Non-	+0.8406 Inhibitor	+0.7315 Inhibitor	-0.9026 Non-inhibitor	-0.9232 Non-inhibitor	-0.9724 Non-Inhibitor	-0.6844 Non-

				Inhibitor						inhibitor
CYP450 1A2 Inhibitor	-0.5548 Non-inhibitor	-0.6655 Non-Inhibitor	+0.5800 Inhibitor	+0.9107 Inhibitor	+0.8658 Inhibitor	+0.6485 Inhibitor	-0.9046 Non-Inhibitor	-0.8240 Non-Inhibitor	-0.8383 Non-Inhibitor	-0.8158 Non-inhibitor
CYP450 3A4 Inhibitor	-0.9773 Non-inhibitor	-0.6661 Non-Inhibitor	-0.9409 Non-Inhibitor	-0.9295 Non-Inhibitor	+0.7552 Inhibitor	-0.8396 Non-inhibitor	-0.9088 Non-inhibitor	-0.9402 Non-inhibitor	-0.9702 Non-Inhibitor	-0.7506 Non-inhibitor
CYP450 2C9 Inhibitor	-0.9329 Non-inhibitor	-0.7837 Non-inhibitor	-0.7951 Non-Inhibitor	-0.8972 Non-Inhibitor	+0.6980 Inhibitor	+0.5676 Inhibitor	-0.9071 Non-inhibitor	-0.9419 Non-inhibitor	-0.9763 Non-Inhibitor	-0.8075 Non-inhibitor
CYP450 2D6 Inhibitor	-0.9502 Non-inhibitor	-0.8486 Non-inhibitor	-0.9458 Non-inhibitor	-0.9545 Non-inhibitor	-0.7553 Non-Inhibitor	-0.8931 Non-Inhibitor	-0.9230 Non-inhibitor	-0.9412 Non-inhibitor	-0.9546 Non-inhibitor	-0.9162 Non-inhibitor
Excretion										
Biodegradation	+0.9500 B	-0.5250 NB	-0.5750 NB	+0.9750 B	-0.8250 NB	-0.5000 NB	+0.5250 B	+1.0000 B	+0.7500 B	+0.8250 NB
AMES Mutagenesis	-1.0000 Non-Ames toxic	-0.7300 Non-Ames toxic	-0.9000 Non-Ames toxic	-0.9900 Non-Ames toxic	-0.7400 Non-Ames toxic	-0.7300 Non-Ames toxic	-0.8700 Non-Ames toxic	-1.0000 Non-Ames toxic	-0.9800 Non-Ames toxic	-0.5000 Non-Ames toxic
Acute Oral Toxicity	III 0.8589	III 0.6711	III 0.8555	IV 0.8289	III 0.5041	III 0.7105	III 0.8552	IV 0.6451	III 0.8487	III 0.5190
Eye irritation (YES/NO)	Yes	Yes	Yes	Yes	No	Yes	Yes	No	Yes	No

Eye corrosion (YES/NO)	Yes	No	Yes	Yes	No	No	Yes	No	Yes	No
hERG inhibition	-0.5865 No	-0.6951 No	-0.5000 No	-0.3944 No	-0.3744 No	-0.5647 No	-0.4331 No	-0.5933 No	-0.8459 No	-0.5729 No
Hepatotoxicity	-0.5359 No	-0.5000 No	-0.6500 No	-0.7625 No	-0.6125 No	-0.6625 No	-0.9000 No	-0.9875 No	-0.6277 No	-0.5750 No
Carcinogenicity (Yes/No)	-0.6000 No	-0.8300 No	-0.6500 No	-0.7035 No	-0.9118 No	-0.8000 No	-0.6600 No	-0.8300 No	+0.5451 Yes	-0.9413 No

L1- Lutein L2- all-trans-Neoxanthin L3- Isoorientin L4- alpha-Carotene L5- Violaxanthin L6- Epigallocatechin_gallate L7- Luteolin_7-O-glucoside L8- Hyperoside L9- Fucosterol L10- Stigmasterol L11- Astragalin L12- Cholest-5-en-3-ol L13- Orientin L14- Ellagic_acid L15- 7-Ketocampesterol L16- Morin L17- Quercetagetin L18- 7-Ketositosterol L19- Flavylium L20- Gossypetin L21- Kaempferol L22- Quercetin L23- 24-Ethylcholesterol L24- Scutellarein L25- Diosmetin L26- Biochanin L27- Chrysoeriol L28- Genistein L29- Luteolin L30- Cianidanol L31- 1_3-Dibenzyl_urea L32- Hesperetin L33- 6-Chromanol-2,8-dimethyl-2-(4,8,12-trimethyltridecyl) L34- Niazirin L35- Cryptochlorogenic_acid L36- Neochlorogenic_acid L37- L45- alpha-Humulene L38- lycopene L39- Bisabolol L40- epiglobulol L41- Carvacrol L42- ferulic_acid L42- caffeic_acid L43- Carvone L44- Nerolidol L45- Thymol L46- p-coumaric_acid L47- Sinapic acid L48- Gamma tocopherol L49- Phytol L50-roridin

3.4. *Drug-Likeness of Selected Phytochemicals with Standards*

The evaluation of drug-likeness for the selected phytochemicals was based on Lipinski's Rule of Five (RO5), which provides guidelines for assessing the oral bioavailability of drug-like compounds (Lipinski, 2004). According to this rule, an orally active drug should have a molecular weight of 500 g/mol or less, an octanol-water partition coefficient (Log P) of no more than 5, and a maximum of 10 hydrogen bond acceptors and 5 hydrogen bond donors. A compound is considered drug-like if it does not exceed more than one of these limits. As shown in Table 3.4, several compounds have high molecular weights exceeding 500 Da, such as lutein (568.87 Da), all-trans-neoxanthin (600.87 Da), violaxanthin (600.87 Da), alpha-carotene (536.87 Da), lycopene (536.87 Da), and roridin (530.61 Da). These compounds often violate Lipinski's Rule of Five (RO5), suggesting possible challenges in oral bioavailability.

Moderate to high molecular weight compounds (300-500 Da) include isoorientin, epigallocatechin gallate, luteolin 7-O-glucoside, hyperoside, astragalin, orientin, cryptochlorogenic acid, and hydrocortisone. Some of these, like epigallocatechin gallate and isoorientin, violate RO5, indicating potential issues with permeability and absorption, while others, such as hydrocortisone, adhere to the rule and may have better drug-like properties. Compounds with low molecular weights (<300 Da) generally show good drug-likeness and

oral bioavailability. This category includes well-known bioactive flavonoids and phenolic acids such as morin, quercetin, kaempferol, diosmetin, epicatechin, biochanin, genistein, luteolin, hesperetin, caffeic acid, ferulic acid, and theophylline. Their lower molecular weight and favorable hydrogen bond donor/acceptor properties make them potential candidates for further pharmacological studies.

Highly lipophilic compounds (miLogP > 5), such as 24-ethylidenelophenol, sitostanol, fucosterol, cholest-5-en-3-ol, 24-ethylcholesterol, poriferasterol, and 28-isoavenasterol, may have poor aqueous solubility but could exhibit good membrane permeability. On the other hand, smaller lipophilic molecules with miLogP values between 2 and 5, including flavylium, bisabolol, nerolidol, thymol, carvacrol, carvone, and 1,3-dibenzyl urea, might strike a balance between permeability and solubility, making them more favorable for drug development.

Table 3.4 Drug Likeness analysis for phytochemicals from *Moringa oleifera*

Compounds	Heavy Atoms(HA)	Molecular weight (MW)	RO5 Violation	Hydrogen Bond Donor (HBD)	Hydrogen Bond Acceptor (HBA)	miLogp
Lutein	42	568.87	3	2	2	1.01
all-trans-Neoxanthin	44	600.87	2	3	4	0.44
Isoorientin	32	448.38	2	8	11	-2.51
alpha-Carotene	40	536.87	2	0	0	0.70
Violaxanthin	44	600.87	2	1	1	0.87
Epigallocatechin_gallate	33	458.37	2	8	11	-0.44
Luteolin_7-O-glucoside	32	448.38	2	7	11	-2.10
24-Ethylidenelophenol	31	426.72	1	1	1	6.82
Hyperoside	33	464.38	2	8	12	-2.59
Sitostanol	30	416.72	1	1	1	6.88
Fucosterol	30	412.69	1	1	1	6.62
Astragalin	32	448.38	2	7	11	-2.10
Cholest-5-en-3-ol	28	386.6	1	1	1	6.34
Orientin	32	448.38	2	8	11	-2.51
Ellagic_acid	22	302.19	0	4	8	0.14
Ketocampesterol	30	414.66	1	1	2	5.50
Morin	22	302.24	0	5	7	-0.56
Quercetagetin	23	318.24	1	6	8	-1.08
Ketositosterol	31	428.69	1	1	2	5.70
Flavylium	16	207.25	0	0	1	3.28
Gossypetin	31	318.24	1	6	8	-1.08
Kaempferol	21	286.24	0	4	6	-0.03
Quercetin	22	302.24	0	5	7	-0.56
24-Ethylcholesterol	30	414.71	1	1	1	6.73
Poriferasterol	30	412.69	1	1	1	6.62

Scutellarein	21	286.24	0	4	6	-0.03
Diosmetin	22	300.26	0	3	6	0.22
(-)-Epicatechin	21	290.27	0	5	6	0.24
Biochanin	21	284.26	0	2	5	0.77
Chrysoeriol	22	300.26	0	3	6	0.22
Genistein	20	270.24	0	3	5	0.52
Luteolin	21	286.24	0	4	6	-0.03
Cianidanol	21	290.27	0	5	6	0.24
1_3-Dibenzyl_urea	18	240.30	0	2	1	2.93
Hesperetin	22	302.28	0	3	6	0.41
6-Chromanol-2,8-dimethyl-2-(4,8,12-trimethyltridecyl)	29	402.6	1	1	2	5.74
Niazirin	20	279.29	0	3	6	-0.51
Cryptochlorogenic_acid	25	354.31	1	6	9	-1.05
alpha-Humulene	15	204.35	1	0	0	4.53
Lycopene	40	536.87				
Bisabolol	16	222.37	0	1	1	3.56
Carvacrol	11	150.22	0	1	1	2.76
ferulic_acid	14	194.18	0	2	4	1.00
caffeic_acid	13	180.16	0	3	4	0.70
Carvone	11	150.22	0	0	1	2.10
Nerolidol	16	222.37	0	1	1	3.86
Thymol	11	150.22	0	1	1	2.76
p-coumaric_acid	12	164.16	0	2	3	1.28
Sinapic acid	16	224.21	0	2	5	0.73
Gamma tocopherol	30	416.68	1	1	2	5.94
Phytol	21	296.53	1	1	1	5.25
Roridin	38	530.61	1	1	9	1.31
28-isoavenasterol	34	468.75	1	0	2	6.98
Hydrocortisone	26	362.46	0	3	5	1.39
Theophylline	13	180.16	0	1	3	-0.52

3.5. Bioactivity test of the selected ligands and standard drug

The bioactivity properties of all selected hit compounds, along with the standard drugs, were determined using established equations 1-4 . The results, as presented in Tables 3.5 and 3.6, indicate that the ligand efficiency (LE) of the analyzed compounds falls within the recommended range of ≥ 0.3, while the fit quality (FQ) values meet the acceptable threshold of ≥ 0.8. Additionally, the ligand-efficiency-dependent lipophilicity (LELP) values for the selected compounds are within the optimal range of -10 to 10, confirming their potential as viable drug candidates. (Abdul-Hammed *et al.*, 2021). The bioactivity analysis of hit compounds from Moringa oleifera against the S-Nitrosoglutathione Reductase receptor (PDB

ID: 3QJ5) highlights a range of promising bioactive molecules with varying ligand efficiency (LE), fractional quality (FQ), and lipophilicity (LOG P) as shown in Table 3.5. Among the most notable compounds, fucosterol, sitostanol, and cholest-5-en-3-ol demonstrated strong activity, with moderate LE values (0.3) and acceptable LELP scores, indicating favorable ligand efficiency. Flavonoids and polyphenols such as ellagic acid, morin, quercetagetin, and quercetin also exhibited significant activity. These compounds generally had better LE values (~0.3-0.4) and higher HA counts, making them favorable candidates for further investigation. Similarly, other flavonoids like diosmetin, biochanin, genistein, and luteolin showed slightly lower activity but maintained strong LE scores and acceptable lipophilicity. Among non-flavonoid compounds, 1,3-dibenzyl urea and hydrocortisone demonstrated reasonable activity with good LE (0.3-0.4) and log P values near 1, indicating balanced hydrophilicity and lipophilicity. The data suggest that sterols and flavonoids contribute significantly to the bioactivity of Moringa oleifera phytochemicals, with their structural diversity influencing ligand efficiency and pharmacokinetic properties.

The bioactivity analysis of hit compounds from Moringa oleifera against the Interleukin-13 receptor in complex with Tralokinumab (PDB ID: 5L6Y) as shown in Table 3.6. Among the top-scoring compounds, fucosterol exhibited the highest activity, followed by ketocampesterol. These sterols displayed moderate LE values (0.2–0.3), suggesting a balance between molecular efficiency and target binding. Flavonoids such as flavylium and luteolin also showed significant activity, with relatively higher LE values (~0.5), indicating strong efficiency despite their moderate molecular weight. Similarly, sitostanol and other sterols, including 24-ethylidenelophenol, ketositosterol, and poriferasterol, demonstrated promising potential, albeit with slightly lower LE values (~0.2–0.3). Hydrocortisone and theophylline, included as standards, exhibited significantly weaker activity. Theophylline displayed the highest LE (0.6) but had limited effectiveness as an inhibitor.

$$Ligand\ Efficiency\ (LE) = -(B.E) \div Heavy\ atoms\ (H.A) \quad (1)$$

$$L.E\ scale = 0.873e - 0.026 \times H.A - 0.064 \quad (2)$$

$$FQ = LE \div LEscale \quad (3)$$

$$LELP = LogP \div LE \quad (4)$$

Table 3.5: Bioactivity analysis of hit compounds and standard for S-Nitrosoglutathione Reductase receptor (PDB ID:3QJ5)

Compound	Binding affinity	Inhibition constant	HA	LE	LE-SCALE	FQ	LOGP	LELP
Fucosterol	-8.8	0.35	29	0.3	0.3	0.9	0.34	1.0
Sitostanol	-8.7	0.42	30	0.3	0.3	0.9	-0.31	-1.2
Cholest-5-en-3-ol	-8.6	0.5	32	0.3	0.3	0.9	1	2.8
Ellagic_acid	-8.5	0.6	22	0.4	0.4	0.9	0.7	2.0
Ketocampesterol	-8.4	0.70	30	0.3	0.3	0.8	0.71	2.5
Morin	-8.4	0.70	30	0.3	0.3	0.8	1	2.9
Quercetagetin	-8.4	0.70	30	0.3	0.3	0.8	0.71	2.5
Ketositosterol	-8.3	0.83	31	0.3	0.3	0.8	1.08	2.3
Flavylium	-8.3	0.83	31	0.3	0.3	0.8	1	2.9
Gossypetin	-8.3	0.83	31	0.3	0.3	0.8	0.71	2.5
Kaempferol	-8.3	0.83	31	0.3	0.3	0.8	1.08	2.3
Quercetin	-8.3	0.83	31	0.3	0.3	0.8	1	2.9
24-Ethylcholesterol	-8.3	0.83	31	0.3	0.3	0.8	0.71	2.5
Poriferasterol	-8.2	0.98	30	0.3	0.3	0.8	1.08	2.3
Scutellarein	-8.2	0.98	30	0.3	0.3	0.8	1	2.9
Diosmetin	-8.1	1.2	21	0.4	0.4	0.9	1	3.0

Biochanin	-8	1.4	21	0.4	0.4	0.9	1	3.0
Chrysoeriol	-8	1.4	22	0.4	0.4	0.9	1	3.0
Genistein	-8	1.4	20	0.4	0.5	0.9	1	3.0
Luteolin	-8	1.4	21	0.4	0.4	0.9	1	3.0
Cianidanol	-7.9	1.6	21	0.4	0.4	0.9	1	3.0
1_3-Dibenzyl_urea	-7.8	1.9	18	0.4	0.5	0.9	1	3.0
Hesperetin	-7.8	1.9	22	0.4	0.4	0.8	1	3.0
6-Chromanol-2,8-dimethyl-2-(4,8,12-trimethyltridecyl)	-7.8	1.9	29	0.3	0.3	0.8	1	3.0
Hydrocortisone	-7.8	1.9	26	0.3	0.4	0.8	1	3.0

Table 3.6: Bioactivity analysis of hit compounds and standard for Interleukin-13 in complex with Tralokinumab receptor (PDB ID:5L6Y)

Compound	Binding affinity	Inhibition constant	HA	LE	LE-SCALE	FQ	LOGP	LELP
Fucosterol	-7.7	2.3	30	0.3	0.3	0.8	0.24	2.8
Ketocampesterol	-7.5	3.2	30	0.3	0.3	0.7	-0.25	-0.4
Flavylium	-7.2	5.3	16	0.5	0.5	0.9	1	2.8
Luteolin	-7.2	5.3	21	0.5	0.5	0.9	0.34	1.0
Sitostanol	-7.1	6.3	30	0.2	0.4	0.8	-0.31	-1.2
24-Ethylidenelophenol	-7	7.4	31	0.2	0.3	0.7	1	2.8

Ketositosterol	-7	7.4	31	0.2	0.3	0.7	1	2.8
Poriferasterol	-7	7.4	31	0.2	0.3	0.7	1	2.8
Hydrocortisone	-6.1	33.9	26	0.2	0.4	0.6	0.71	2.5
Theophylline	-4.4	597.1	13	0.6	0.6	0.9	1.08	2.3

3.6. Oral bioavailability Analysis of the selected ligands and standard

The selected compounds with favorable ADMET and drug-likeness properties and those exhibiting promising characteristics were further evaluated for oral bioavailability. The oral bioavailability parameters were assessed using the SwissADME online tool (Daina *et al.*, 2017).. Figureure 2 illustrates the optimal bioavailability range for key properties, including Lipophilicity (LIPO), Molecular Size (SIZE), Polarity (POLAR), Solubility (INSOLU), Unsaturation (INSATU), and Flexibility (FLEX) (Daina *et al.*, 2017).

The recommended thresholds for these properties are as follows: molecular weight ≤500 g/mol (SIZE), topological polar surface area (TPSA) between 20–130 Å² (POLAR), octanol–water partition coefficient (XLOGP3) within −0.7 to 5.0 (LIPO), solubility (ESOL Log S) ≤6.0 (INSOLU), fraction of sp^3 carbons (Csp^3) ≥0.25 (INSATU), and rotatable bonds ≤10 (FLEX) (Daina *et al.*, 2017).. As shown in Table 3.7, all hit compounds demonstrated favorable oral bioavailability parameters, with the exception of some deviations in TPSA values.

Table 3.7 Oral bioavailability for selected ligands and standard

LIGANDS	Formular	Mass	TPSA	#Rotatable bonds	XLOGP3	WLOGP	ESOL Log S	Lipinski #violations	Bioavailability Score	PAIN #alerts	Fraction Csp3	Synthetic Accessibility
Fucosterol	$C_{29}H_{48}O$	412.69	20.23	5	8.85	7.94	-7.64	1	0.55	0	0.86	6.15
Cholest-5-en-3-ol	$C_{27}H_{46}O$	386.65	20.23	5	8.72	7.39	-7.40	1	0.55	0	0.93	5.98
Ketocampesterol	$C_{16}H_{12}O_7$	414.66	37.30	5	7.73	6.81	-6.95	1	0.55	0	0.89	6.10
Ketositosterol	$C_{29}H_{48}O_2$	428.69	37.30	6	8.27	7.20	-7.31	0	0.55	0	0.90	6.23
Poriferasterol	$C_{29}H_{48}O$	412.69	20.23	5	8.85	7.94	-7.64	1	0.55	0	0.86	6.15
Luteolin	$C_{15}H_{10}O_6$	286.24	113.13	1	2.53	2.28	-3.71	0	0.55	0	0.00	3.02
24-Ethylcholesterol	$C_{29}H_{50}O$	414.71	20.23	6	9.34	8.02	-7.90	1	0.55	0	0.93	6.30
Scutellarein	$C_{15}H_{10}O_6$	286.24	111.13	1	2.66	2.28	-3.79	0	0.55	1	0.00	3.04
Diosmetin	$C_{16}H_{12}O_6$	300.26	100.13	2	3.10	2.59	-4.06	0	0.55	0	0.06	3.05
Biochanin	$C_{16}H_{12}O_{15}$	284.26	79.90	2	2.99		-3.78	1	0.55	0	0.29	5.12
Genistein	$C_{15}H_{10}O_5$	270.24	90.90	1	2.67	2.58	-3.72	0	0.55	0	0.00	2.87
Cianidanol	$C_{15}H_{14}O_6$	290.27	120.38	1	0.36	1.22	-2.22	0	0.55	1	0.20	3.50
Hesperetin	$C_{21}H_{20}O_{10}$	302.28	96.22	2	2.60	2.19	-3.62	1	0.55	0	0.19	3.22
Hydrocortisone	$C_{21}H_{30}O_5$	362.46	94.83	2	1.61	1.78	-2.97	0	0.55	0	0.81	5.16
Theophylline	$C_7H_8N_4O_2$	180.16	72.68	0	-0.02	-1.0	-1.46	0	0.55	0	0.29	1.87

Fucosterol Ketocampesterol Luteolin

Flavylium Luteolin Sitostanol

24-Ethylidenelophenol Ketositostanol Porifersterol

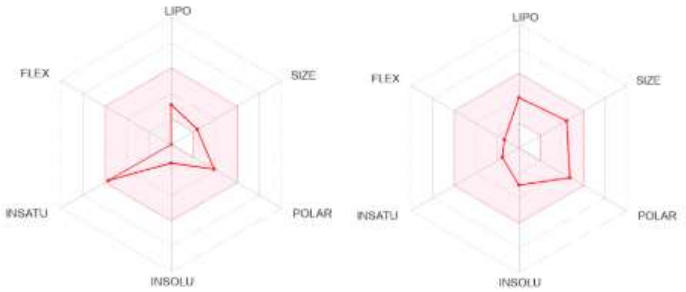

Theophylline Hydrocortisone

Figure 2: Bioavailability radar of the selected compounds from Moringa oleifera and standards

3.7. Binding Mode and Molecular Interactions of the Best Hit Compound and the Standards

The docking study revealed that the hit compounds from Moringa oleifera interacted with key residues of GSNOR, particularly within its active site, through hydrogen bonding and hydrophobic interactions (Table 3.8). Several ligands demonstrated interactions with residues essential for enzymatic function, including His 66, Cys 44, Cys 173, Gln 111, Gln 117, Lys 227, and Asp 55, which contribute to enzyme stability, substrate recognition, and catalytic activity. Fucosterol formed hydrogen bonds with Gln 111, Lys 227, Asn 270, and Asn 224, while also engaging in hydrophobic interactions with Ala 317, Val 293, Tyr 139, His 66, Cys 173, and Phe 318. The interaction with His 66 and Cys 173 is particularly notable, as these

residues coordinate with structural zincs necessary for enzymatic function. Cholest-5-en-3-ol also interacted with Gln 111, Asp 55, Gln 117, and Asn 279, reinforcing its presence in the active site. Ketocampesterol and Ketositosterol formed hydrogen bonds with Gln 111, Asp 55, Asn 270, and Gln 117, while their hydrophobic interactions with Ile 249, Val 221, Phe 197, and Cys 267 provided additional stability. These interactions suggest their potential to interfere with the enzyme's normal function. Poriferasterol, another active ligand, formed hydrogen bonds with Asp 55, Gln 111, Gln 117, Lys 227, and Asn 224, while also engaging in hydrophobic interactions with Thr 177, Val 291, Phe 318, and Tyr 92, further stabilizing its binding. Luteolin, Scutellarein, and Diosmetin, flavonoid-based compounds, displayed strong hydrogen bonding with Lys 227, Asp 222, and Gln 117, along with interactions involving Thr 46, Val 293, Ile 268, Cys 267, and His 45, which are crucial for maintaining the enzyme's active conformation. Notably, Luteolin and Diosmetin also interacted with Arg 368, suggesting additional stabilization through electrostatic forces. 24-Ethylcholesterol, Biochanin, and Genistein also showed significant interactions with Lys 227, Asn 224, Gln 117, and Met 361, along with hydrophobic interactions involving Val 293, Gly 292, His 45, and Arg 368, reinforcing their potential as inhibitors. Hesperetin and Hydrocortisone displayed similar interaction patterns, forming hydrogen bonds with Met 361, Lys 227, Asn 270, and Asp 55, while engaging in hydrophobic interactions with Thr 46, Gly 120, Gln 117, and Tyr 139. Interestingly, Cianidanol and Theophylline, while forming hydrogen bonds with active site residues, showed comparatively fewer hydrophobic interactions, which may impact their binding stability. Theophylline in particular interacted with Gln 117, Gln 111, Met 361, Lys 227, and Asn 224, but lacked significant engagement with key hydrophobic residues, potentially explaining its weaker binding characteristics.

The docking analysis of Moringa oleifera compounds against IL-13 (PDB ID: 5L6Y) also revealed significant interactions with the receptor's active site residues, particularly Asp 50, Lys 31, Ser 30, Asp 51, Asn 26, Gly 81, and Asp 92, which play crucial roles in charge complementarity and structural stability. Among the compounds, Fucosterol formed hydrogen bonds with Asp 205, Ser 151, Arg 85, Gly 328, Asp 78, and Lys 169, while engaging in hydrophobic interactions with Gly 81, Ser 151, Asp 78, Arg 78, and Met 107. Its interaction with Asp 78 and Gly 81, which are part of the active site, suggests a potential influence on receptor function. Flavylium also demonstrated strong binding through hydrogen bonds with Asn 83, Ser 151, Lys 169, Thr 82, Asp 205, Gly 229, and Thr 228, alongside electrostatic and hydrophobic interactions with Lys 169, Thr 228, Asp 78, Thr 82, Asn 83, Gly 410, Ser 411, and Asp 205, suggesting possible receptor modulation. Similarly, Ketocampesterol interacted via hydrogen bonds with Asp 78, Asp 409, Ser 151, Asp 205, Ser 445, and Thr 228, and engaged in hydrophobic interactions with Ser 445 and Asp 78, indicating a possible inhibitory effect. Luteolin formed hydrogen bonds with Asn 83, Asp 205, Gly 80, Thr 82, Asp 78, Lys 169, and Gly 81, while hydrophobic interactions involved Asn 83, Thr 82, Gly 81, Ser 151, and Lys 169, making it a promising candidate for receptor interference. Poriferasterol primarily engaged Lys 296 and Glu 300 in hydrogen bonding, with additional hydrophobic interactions with Leu 415, Thr 228, Lys 296, Arg 333, Phe 330, and Gly 328, suggesting its potential to alter receptor conformation. Other compounds such as Sitostanol and 24-Ethylidenelophenol displayed weaker interactions with IL-13, with Sitostanol forming hydrogen bonds with Pro 66 and His 218, while hydrophobic interactions involved Ser 69, Tyr 215, Trp 99, Leu 451, Ala 454, Val 91, Val 455, Pro 66, His 218, and Tyr 214. 24-Ethylidenelophenol mainly interacted

with Thr 376, Glu 17, Leu 25, and Glu 372 via hydrogen bonds and showed additional hydrophobic interactions with Gln 24, Thr 376, Glu 372, Leu 25, Ala 21, Ser 373, and Leu 20, indicating a lower likelihood of disrupting receptor activity. Hydrocortisone and Theophylline showed limited interactions, with Hydrocortisone forming a hydrogen bond with Arg 63 and engaging in hydrophobic interactions with Trp 99, Ala 454, Ser 69, Tyr 215, Leu 451, and Val 455, while Theophylline interacted with Asp 78 and Ser 151 through hydrogen bonds and with Asp 205, Asp 78, and Asn 83 electrostatically.

Table 3.9: The Binding mode and Molecular interaction, and Electrostatic/Hydrophobic interactions of hit compounds and standards with S-Nitrososgluthathione receptor (PDB ID:3QJ5)

S/N	Ligands	Binding affinity	3QJ5 Receptor amini acid forming H-bond ligands	Electrostatic/Hydropobic interaction involved	Inhibition constant (Ki), uM
1	Fucosterol	-8.8	Gln 111, Lys 227, Asn 270, Asn 224	Ala 317, Val 293, Val 202, Tyr 139, His 66, Tyr 92, Cys 173, Gly 174, Thr 177, Val 291,Thr 50, Gly 118, Phe 318, Tyr 92, The 46	0.4
2	Cholest-5-en-3-ol	-8.6	Gln 111, Asp 55, Gln 117, Asn 279	Ala 317, Val 293, Val 202, Tyr 139, His 66, Tyr 92, Cys 173, Gly 174, Thr 177, Val 291,Thr 50, Gly 118, Phe 318, Tyr 92, The 46	0.5
3	Ketocampesterol	-8.4	Gln 111, Asp 55, Asn 270, Gln 117	Pro 242, Asn 270, Asn 224, Lys 227, Gly 364, Met 261, Val 273, Ile 249, Phe 197,Val 221, Ile 223, Asp 22, Gly 198, Gly 200, Leu 199, Cys 267	0.7
4	Ketositosterol	-8.3	Lys 227, Asp 222, Asn 224, Gln 111, Gln 117, Asp 55,	Met 361, His 45, Gly 364, Lys 227, Ile 223, Asn 270, Val 221, Val 273, Pro 242, Ile 249, Phe 197, Ile 268, Asp 222, Gly 198, Ley 199Cys 267, Gly 200	0.8
5	Poriferasterol	-7	Asp 55, Gln 111, Gln 117, Lys	Thr 177, Thr 316, Val 291, Phe 318, Ala 317, Ile 93, Gln 117, His 138,	1.0

			227, Asn 224	Gly 120, Asp 55, Glu 57, Gly 118, Tyr 139, Gly 141, Val 293, Thr 46, Tyr 92	
6	Luteolin	-7.2	Lys 227, Asp 222, Gln 117	Thr 46, Val 293, Ile 268, Cys 267, Met 361, His 45, Arg 368, Cys 44, Thr 177, Phe 318, , Ala 317, Gly 319, Tyr 92	1.4
7	24-Ethylcholesterol	-8.3	Asn 224, Lys 227, Gln 117, Met 361	Val 293, Gly 292, His 45, Cys 44, Arg 368, Met 361, Thr 46, Thr 177, Val 291, Tyr 92, Gly 174, Ile 268, Cys 267, Val 202, Gly 201, Ile 367, Ser 366	1.0
8	Scutellarein	-8.2	Lys 227, Asn 224, Asp 222, Asp 55	Thr 177, Val 291, Ile 268, Cys 267, His 45, His 362, Lys 227, Gly 364, Met 361, SER366, Gly 201, Gly 200	1.0
9	Diosmetin	-8.1	Asp 55, Asn 270, Lys 227, Asn 224, Met 361	Arg368, His 45, Arg 368, Val 202, Ile 268, Cys 267, Gly 292, Val 291, Thr177,Thr 316, Ala 317, Gly 319, Tyr 92, Phe 318, Cys 44, Cys 173	1.2
10	Biochanin	-8	Lys 227, Asn 224, Asn 270, Asp 222, Met 361	Thr 177, Val 291, Gly 292, Val 293, Val 202, Cys 2667, His 45, Gly 201, Gly 200, Ser 366, Lys 227, Gly 364	1.4
11	Genistein	-8	Lys 227, Met 361, Asp 222, Asn 224	Val 293, Val 291, Gly 292, Val 202, Cys 267, Cys 44, Arg 368, Gly 200, Ile 268, Ile 367, Gly 201, Met 361, Gly 364	1.4
12	Cianidanol	-7.9	Leu 25, His 380, Thr 376, Glu 17,	His 66, Tyr 92, Gln 117, Gly 141, Gly 120, His 138, Leu 137, Val 62, Cys 59, Thr 50, Leu 64, Thr 50, Glu 57, Gly 58, Tyr 139, Thr 46	1.6

13	Hesperetin	-7.8	Met 361, Lys 227, Asn 270, Asp 55	Thr 46, Asp 55, Gly 58, Glu 57, Cys 59, Leu 64, Thr 50, Val 62, Leu 137, His 138, Gly 120, Gln 117, Fly 118, Gly 141, Tyr 139, Tyr 92, His 66	1.9
13	**Hydrocortisone**	-7.8	Asn 270, Lys 227, Gln 111, Asp 55, ,Met 361	Gly 203, Gly 200, Ile 268. Leu 1999, Gly 198, Asp 22, Ile 223, Asn 224, Lys 227, Gly 364, Gly 201, Met 361, Arg 368, Val 202, His 45,	1.9
13	**Theophylline**	-5.5	Gln 117, Gln 111, Met 361, Lys 227, Asn 224	His 45, Met 361, Gly 364, Ser 366, Ile 367, Gly 201, Arg 368, Gly 200, Val 202	66.6

Table 3.10: The Binding mode and Molecular interaction, and Electrostatic/Hydrophobic interactions of hit compounds and standards with Tralokinmunab receptor (PDB ID:5L6Y)

S/N	Ligands	Binding affinity	5L6Y Receptor amini acid forming H-bond ligands	Electrostatic/Hydropobic interaction involved	Inhibition constant (Ki), uM
1	Fucosterol	-7.7	Asp 205, Ser 151, Arg 85, Gly 328, Asp 78, Lys 169	Gly 81, Ser 151, Asp 78, Arg 78, Met 107	0.4
2	Flavylium	-7.2	Asn 83, Ser 151,Lys 169, Thr 82, Asp 205,Gly 229, Thr 228,	Lys 169, Thr 228, Asp 78, Thr 82, Asn 83, Gly 410, Ser 411, Asp 205	0.5
3	Ketocampesterol	-7.5	Asp 78, Asp 409, Ser 151, Asp 205,	Ser 445, Asp 78	0.7

			Ser 445, Thr 228		
4	Luteolin	-7.2	Asn 83, Asp 205, Gly 80, Thr 82, Asp 78, Lys 169, Gly 81	Asn 83, Thr 82, Gly 81, Ser 151, Lys 169	0.8
5	Poriferasterol	-7	Lys 296, Glu 300,	Leu 415, Thr 228, Lys 296, Arg 333, Phe 330, Gly 328	1.0
6	Sitostanol	-7.1	Pro 66, His 218	Ser 69, Tyr 215, Trp 99, Leu 451, Ala 454, Val 91, Val 455, Pro 66, His 218, Tyr 214	1.4
7	24-Ethylidenelophenol	-7	Thr 376, Glu 17, Leu 25, Glu 372,	Gln 24, Thr 376, Glu 372, Leu 25, Ala 21, Ser 373, Leu 20	1.0
8	**Hydrocortisone**	-6.1	Arg 63,	Trp 99, Ala 454, Ser 69, Tyr 215, Leu 451, Val 455	1.0
9	**Theophylline**	-4.4	Asp 78, Ser 151	ASP 205, Asp 78, Asn 83	1.2

Figure 3:Binding mode and molecular interactions of the selected hits and standard with S-Nitrososgluthathione receptor (PDB ID:3QJ5)

Ligands	Binding Mode	Interaction
Fucosterol	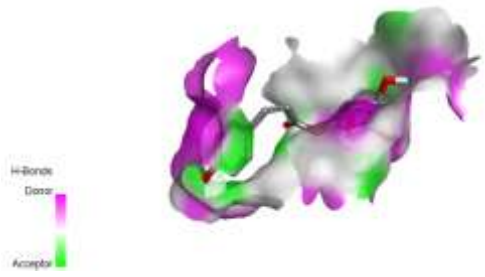	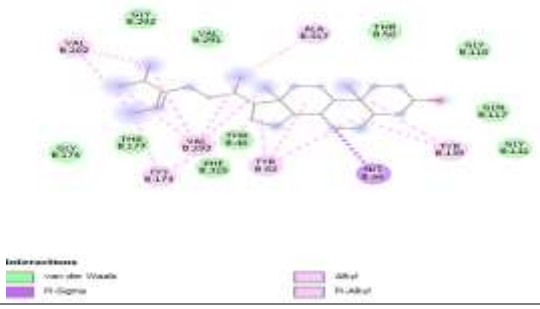

Cholest-5-enol

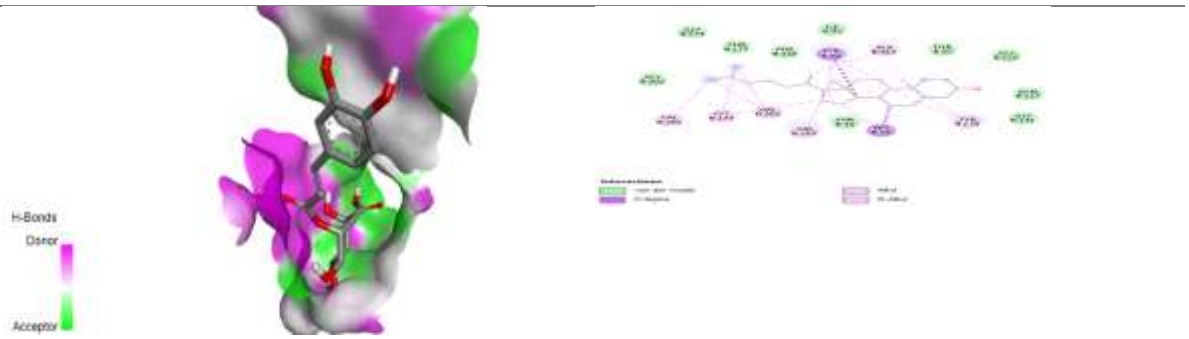

Ketocampestanol

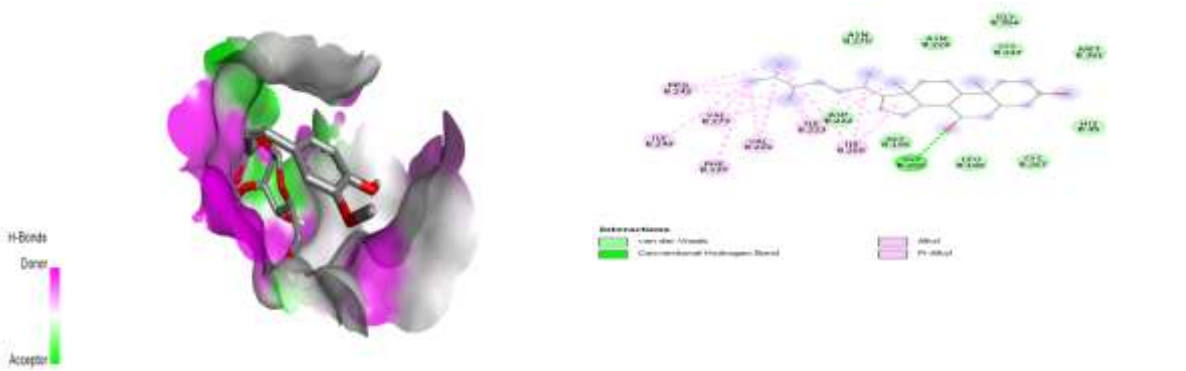

Ketositostanol

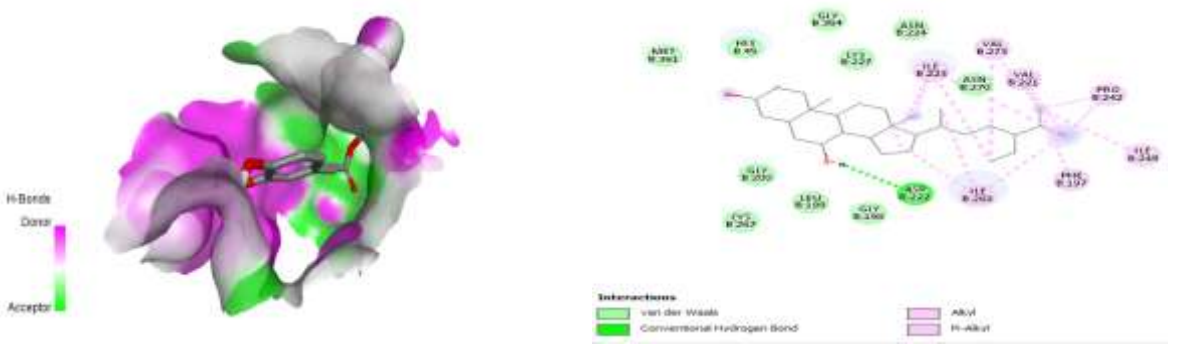

Hydrocortisone

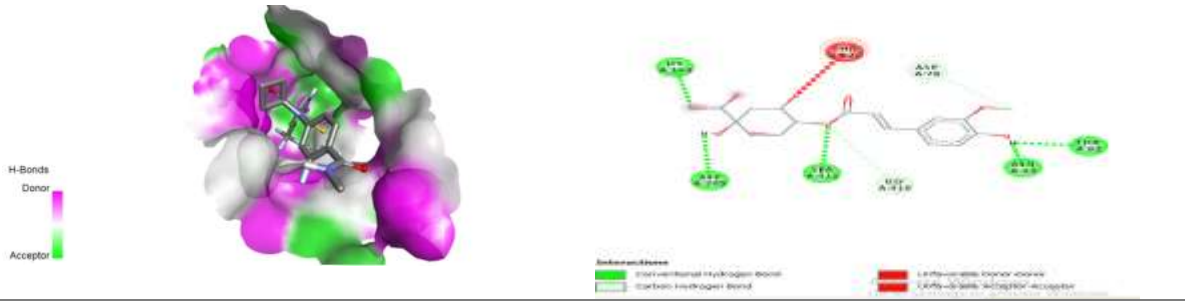

Theophylline	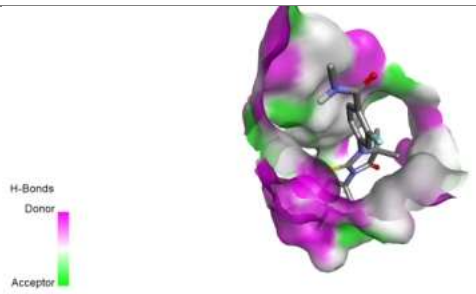		

Figure 4: Binding mode and molecular interactions of the selected hits and standard against Interleukin-13 in complex with Tralokinumab receptor (PDB ID:5L6Y)

Ligands	Binding Mode	Interaction
Flavylium	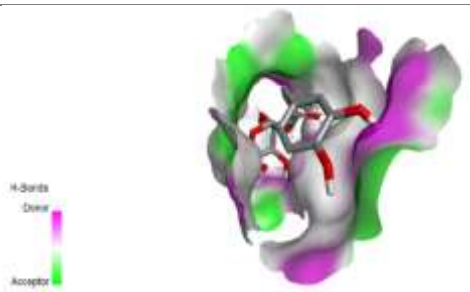	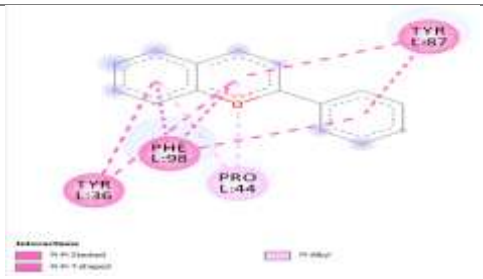
Fucosterol	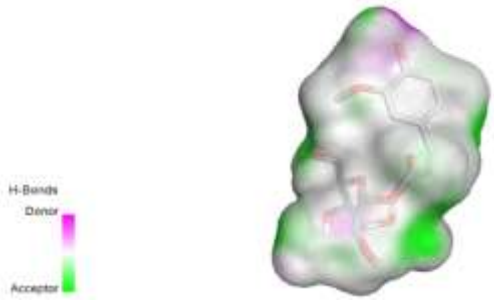	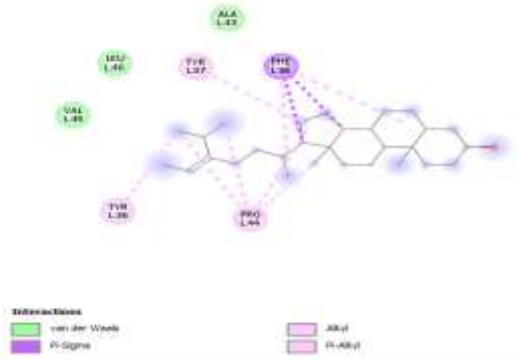
Luteolin	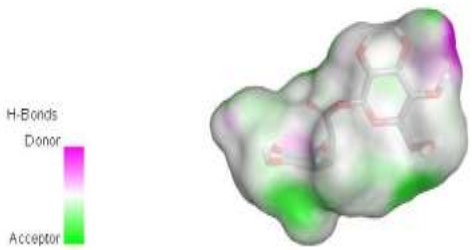	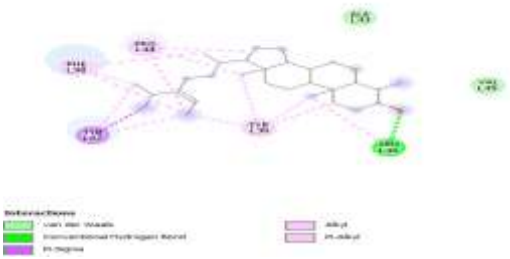

Hydrocortisone

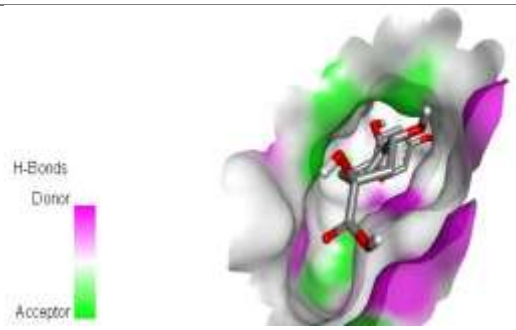

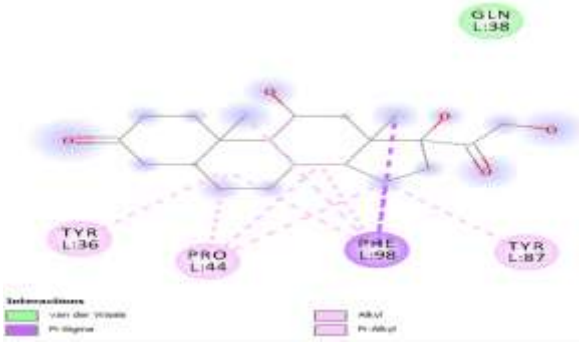

Theophylline

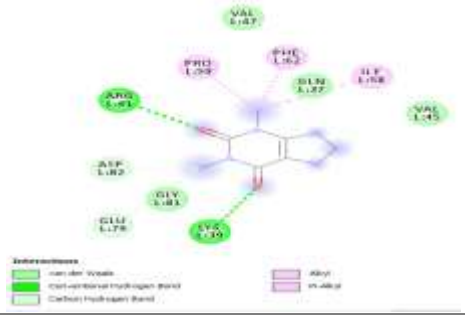

4. **Conclusion**

This study evaluated one hundred and seventy-seven (177) phytochemicals isolated from Moringa oleifera against S-Nitrosoglutathione Reductase (GSNOR, PDB ID: 3QJ5) and Interleukin-13 (IL-13, PDB ID: 5L6Y) through in silico studies (structure-based drug design). The results obtained revealed that Fucosterol (-8.8 kcal/mol), Cholest-5-en-3-ol (-8.6 kcal/mol), Ketocampesterol (-8.4 kcal/mol), and Ketositosterol (-8.3 kcal/mol) share the same pocket with GSNOR by interacting with His 66, Cys 44, Cys 173, Gln 111, and Gln 117, which are essential for enzyme function. These interactions suggest their potential as competitive inhibitors of GSNOR, interfering with enzymatic stability and catalytic activity. Similarly, Fucosterol (-7.7 kcal/mol), Luteolin (-7.2 kcal/mol), and Flavylium (-7.2 kcal/mol) were found to share the same pocket with IL-13 by interacting with Asp 78, Gly 81, and Lys 169, which play crucial roles in receptor activation and structural stability. These interactions indicate their potential for modulating IL-13 function, making them strong candidates for further investigation. These ligands exhibit favorable ADMET properties, drug-likeness, oral bioavailability, and biological activity profiles. Therefore, they represent promising inhibitors of GSNOR and IL-13, with potential applications in drug development. Their properties and activity can be further optimized during lead development for enhanced therapeutic efficacy

REFERENCES

Abdul-Hammed, M., Adedotun, I.O., Falade, V.A. and Adepoju, A.J. (2021). Target-based drug discovery, ADMET profiling and bioactivity studies of antibiotics as potential inhibitors of SARS-CoV-2 main protease (Mpro). *Virus Dis*., 32, 642–656.

Adedotun, I.O., Abdul-Hammed, M., Hamzat, B.A., Akinboade, M.W., Afolabi, T.I., and Ismail, U.T. (2022). Molecular docking, ADMET analysis, and bioactivity studies of phytochemicals from Phyllanthus niruri as potential inhibitors of hepatitis C virus NSB5 polymerase. *Journal of the Indian Chemical Society, Elsevier*. **99:** 100321

Adigwe, O.P., Ibrahim, J.A., Gegele, I.B., Adzu, B. and Yetunde Isimi, C., 2022. Medicinal Plants Used for Management of Asthma in FCT, Abuja and Its Environs. *European Journal of Medicinal Plants*, *33*(1), pp.8-38.

Anuragi, H., Singhal, R.K., Tanveer, Y., Yasmin, H., Srijan, A., Bharati, A., Chand, L., Taria, S., Rajarajan, K., Ram, A. and Handa, A.K. (2022). The Primacy of Moringa (Moringa oleifera Lam.) in Boosting Nutrition Status and Immunity Defence Amidst the COVID-19 Catastrophe: A Perspective. Phyton (0031-9457), 91(9).

Barnes, P. J. (2022). Glucocorticosteroids: Current and future directions. *British Journal of Pharmacology, 179*(5), 1023–1038. https://doi.org/10.1111/bph.15750

Barnett, S. D., and Buxton, I. L. O. (2017). The role of S-nitrosoglutathione reductase (GSNOR) in human disease and therapy. Critical Reviews in Biochemistry and Molecular Biology, 52(3), 340–354. https://doi.org/10.1080/10409238.2017.1304353

BIOVIA, S. D. 'Discovery Studio Visualizer, version 20.1', San Diego Dassault Systèmes, (2019).

Cheng, F., Li, W., Zhou, Y., Shen, J., Wu, Z., Liu,G., Lee, P., Tang, Y. 'admetSAR: A Comprehensive Source and Free Tool for Assessment of Chemical ADMET Properties', J. Chem. Inf. Model. 52, 11, pp. 3099–3105, (2012), doi: 10.1021/ci300367a.

Daina, A., Michielin, O., and Zoete, V. (2017). SwissADME: a free web tool to evaluate pharmacokinetics, drug-likeness, and medicinal chemistry friendliness of small molecules. Scientific reports, 7(1), 1-13.

Falade, V. A., Adelusi, T. I., Adedotun, I. O., AbduC-Hammed, M., Lawal, T. A., and Agboluaje, S. A. (2021). In silico investigation of saponins and tannins as potential inhibitors of SARS-CoV-2 main protease (Mpro). In Silico Pharmacology, 9(1), 1-15.

Onawole, A.T., Sulaiman, K.O., Adegoke, R.O., Kolapo, T.U. (2017). Identification of potential inhibitors against the Zika virus using consensus scoring. *J Mol Graph Model.* **73**:54-61.

Lee I, Keum J, Nam H (2019) DeepConv-DTI: Prediction of drug-target interactions via deep learning with convolution on protein sequences. PLoS Comput Biol 15(6): e1007129. https://doi.org/10.1371/journal.pcbi.1007129

Lipinski, C.A. (2004). Lead profiling Lead-and drug-like compounds: the rule of five revolution, Drug Discovery Today, 1(4):337-341

Mahajan, S.G., Banerjee, A. Chauhan, B.F., Padh, H., Nivsarkar, M., Mehta, A.A. (2009). Inhibitory Effect of n-butanol Fraction of Moringa oleifera Lam. Seeds on Ovalbumin-Induced Airway Inflammation in a Guinea Pig Model of Asthma. International Journal of Toxicology.;28(6):519-527. doi:10.1177/1091581809345165

Panettieri, R.A., Sjöbring, U., Péterffy, A., Wessman, P., Bowen, K., Piper, E., Colice, G. and Brightling, C.E. (2018). Interleukin-13 in complex with Tralokinumab for severe, uncontrolled asthma (STRATOS 1 and STRATOS 2): two randomised, double-blind, placebo-controlled, phase 3 clinical trials. The Lancet Respiratory Medicine, 6(7), pp.511-525.

Tian, W., Chen, C., Lei, W., Zhao, J., and Lian, J., 'CASTp 3.0: computed atlas of surface topography of proteins', Nucleic Acids Res. 46, W1, pp. W363–W367, (2018).

Vithi Hitendra Patel, Srijani Thannir, Maulik Dhanani, Ivan Augustine, S. L Sandeep, Abdulrahim Mehadi, Chaithanya Avanthika, Sharan Jhaveri, (2023). Current Limitations and Recent Advances in the Management of Asthma, Disease-a-Month, Volume 69, Issue 7, 101483, ISSN 0011-5029, https://doi.org/10.1016/j. disamonth.2022.101483.

World Health Organization, 2022